0026-895X/03/6302-297–310$7.00
MOLECULAR PHARMACOLOGY
Vol. 63, No. 2
1965/1037461
Mol Pharmacol 63:297–310, 2003
Printed in U.S.A.

Basic Fibroblast Growth Factor Activates Endothelial Nitric-Oxide Synthase in CHO-K1 Cells via the Activation of Ceramide Synthesis

TULLIO FLORIO, SARA ARENA, ALESSANDRA PATTAROZZI, STEFANO THELLUNG, ALESSANDRO CORSARO, VALENTINA VILLA, ALESSANDRO MASSA, FABRIZIO DIANA, GIUSEPPE SPOTO, SABRINA FORCELLA, GIANLUCA DAMONTE, MIRELLA FILOCAMO, UMBERTO BENATTI, and GENNARO SCHETTINI

Pharmacology and Neurosciences, National Institute for Cancer Research c/o Advanced Biotechnology Center, Genova, Italy (T.F., S.A., A.P., S.T., A.C.,V.V., A.M., F.D., G.S.); Department of Oncology, Biology and Genetics, University of Genova, Genova, Italy (S.A., A.P., S.T., A.C., V.V., A.M., F.D., G.S.,); Departments of Biomedical Sciences (T.F.) and Applied Sciences of Oral and Dental Diseases(G.S., S.F.), University G. D'Annunzio, Chieti, Italy; and Department of Experimental Medicine (G.D., U.B.), and Lab. Diagnosi Pre-Postnatale Malattie Metaboliche Istituto G. Gaslini, Genova, Italy (M.F.)

Received July 1, 2002; October 28, 2002

This article is available online at http://molpharm.aspetjournals.org

ABSTRACT

In this study, we analyzed the intracellular mechanisms leading to basic fibroblast growth factor (bFGF)-dependent production of NO in Chinese hamster ovary (CHO)-K1 cells and a possible physiological role for such an effect. bFGF induces NO production through the activation of the endothelial form of NO synthase (eNOS), causing a subsequent increase in the cGMP levels. In these cells, the activation of eNOS by bFGF is Ca^{2+}- and mitogen-activated protein kinase-independent. The translocation of the enzyme from the plasma membrane, where it is located in caveolae bound to caveolin 1, to the cytosol is the crucial step for the synthesis of NO through the eNOS isoform. We demonstrate that bFGF activates a sphingomyelinase to synthesize ceramide, which, in turn, allows the dissociation of eNOS from caveolin 1 and its translocation to the cytosol in the active form, where it catalyzes the synthesis of NO. In fact, drugs interfering with sphingomyelinase activity blocked bFGF activation of eNOS, and an increase in ceramide content was detected after bFGF treatment. Moreover, in fibroblasts derived from patients with Niemann-Pick disease, in which the enzyme is genetically inactive, bFGF is unable to elicit eNOS activation. The NO produced after bFGF treatment, through the activation of guanylyl cyclase and protein kinase G, mediates a mitogen-activated protein kinase-independent cell proliferation. In conclusion, our data show that, in CHO-K1 cells, bFGF regulates the activity of eNOS through a novel intracellular pathway, involving the induction of ceramide synthesis and that the NO released participates in bFGF proliferative activity.

Nitric oxide (NO) is an important intracellular and intercellular mediator involved in the modulation of many physiological processes in different tissues, including blood flow regulation, platelet aggregation, smooth muscle relaxation, apoptosis, central and peripheral neurotransmission, and different neuroendocrine responses (Moncada and Higgs, 1993; Nathan and Xie, 1994).

NO is synthesized by a family of three distinctive isoforms of nitric-oxide synthase (NOS), named after the tissues in which they were originally described. Neuronal and endothelial NOS [nNOS (or NOS I) and eNOS (or NOS III), respectively] are Ca^{2+}/calmodulin-dependent enzymes constitutively expressed not only in neuronal and endothelial cells

This work was supported by grant 99.02482 Ct04 from Consiglio Nazionale delle Ricerche (to T.F.); Italian Association for Cancer Research (2002), MISAN (Targeting of tumoral vessels and antiangiogenic therapy), and European community contract QLG3-CT-1999-00908 (to G.S.).

T.F. and S.A. contributed equally to this work.

The results here reported were presented in part at the Cell Signaling Transcription and Translation as Therapeutic Targets Conference, Luxembourg, Jan 30–Feb 2, 2002.

ABBREVIATIONS: NOS, nitric-oxide synthase; nNOS, neuronal nitric-oxide synthase; eNOS, endothelial nitric-oxide synthase; iNOS, inducible nitric-oxide synthase; cNOS, constitutive nitric-oxide synthase; bFGF, basic fibroblast growth factor; CHO, Chinese hamster ovary; MAP, mitogen activated protein; MEK, mitogen activated protein kinase kinase; PKG, protein kinase G; D609, tricyclo-decan-9-yl xanthate; Ly-83583, 6-(phenylamino)-5,8-quinolinedione; BAPTA/AM, 1,2-bis(2-aminophenoxy)ethane-*N*,*N*,*N*′,*N*′-tetraacetic acid tetra(acetoxymethyl)ester; KT 5823, *N*-methyl-(8*R**,9*S**,11*S**)-(–)-9-methoxy-9-methoxycarbonyl-8-methyl-2,3,9,10-tetrahydro-8,11-epoxy1H,8H,11H-2,7β,11α-triazadibenzo [*a*,*g*]cycloocta[*c*,*d*,*e*]-trinden-1-one; L-NIO, L-N^5-(1-iminoethyl)-ornithine dihydrochloride; CCK, cholecystokinin; NNA, N^{ω}-NO_2-L-arginine; L-NAME, N^G-nitro-L-arginine methylester hydrochloride; U73122, 1-(6-((17-β-3-methoxyester-1,3,5(10)-trien-17-yl)amino)hexyl)-1H-pyrrole-2,5-dione; ERK, extracellular signal-regulated kinase; $[Ca^{2+}]_i$, intracellular Ca^{2+} concentration; DMS, *N*,*N*-dimethyl-sphingosine; S1P, sphingosine 1-phosphate; PTX, pertussis toxin; PD98059, 2′-amino-3′-methoxyflavone; SNP, sodium nitroprusside.

but also in muscle cells, fibroblasts, and various epithelial cells (Nathan and Xie, 1994). They release NO for short periods of time in response to receptor stimulation (Moncada et al., 1991). Inducible NOS [iNOS (or NOS II)] is mainly expressed in macrophages and other blood cells, astrocytes, microglia, and endothelial cells and is transcriptionally activated, in a Ca^{2+}/calmodulin-independent manner, by cytokines and other pro-inflammatory agents (Moncada et al., 1991). Conversely, the activation of the constitutive forms of NOS (cNOS) is almost always strictly Ca^{2+}/calmodulin-dependent; an increase in intracellular Ca^{2+} concentration ($[Ca^{2+}]_i$) induces the formation of active Ca^{2+}-calmodulin complexes that bind with high-affinity specific domains of these enzymes (Moncada et al., 1991; Nathan and Xie, 1994). Beside changes in $[Ca^{2+}]_i$, which represent the crucial cofactor for the activation of cNOS, after receptor-dependent stimulation, different protein kinases and phosphatases may also regulate the activity of these enzymes (Garcia-Cardena et al., 1996; Corson et al., 1996; Fleming and Busse, 1999).

In their inactive configuration, cNOS are bound to specific plasma membrane proteins, from which they are released upon their activation. In particular, nNOS is kept localized to cell membrane compartments by its interaction with the 95-kDa postsynaptic density protein in neurons and to α-syntrophin in muscle cells (Brenman et al., 1996), whereas, in resting cells, eNOS is localized, through myristoylation and palmitoylation, to particular structures of the plasma membrane called caveolae (Feron et al., 1996; Fleming and Busse, 1999). Caveolae are membrane micro-compartments involved in the regulation of endocytosis, Ca^{2+} homeostasis and clustering of GPI-anchored proteins. More recently, caveolae have also been proposed to represent specialized sites for the interaction among signal transduction effectors (Anderson, 1998). Caveolae have a distinct lipid composition because they are highly enriched in sphingolipids, among them ceramides, a class of sphingolipids that act as intracellular second messengers (Anderson, 1998). Ceramides are formed by acylation of sphingosine, induced by the enzyme ceramide synthase, or formed by hydrolysis of sphingomyelin operated by a family of sphingomyelinases (Kolesnick and Fuks, 1995; Hannun, 1996). As far as protein composition, caveolae are characterized by the presence of a family of three integral membrane proteins named caveolin 1, 2, and 3 (Anderson, 1998). Caveolin 1 is surely the most important protein involved in the three-dimensional structure and function of caveolae. In resting cells, caveolin 1 binds the inactive form of eNOS, preventing the catalytic activity of the enzyme and keeping it localized in the caveolae (Garcia-Cardena et al., 1996; Fleming and Busse, 1999). Upon cellular activation (i.e., increase in Ca^{2+} concentration), eNOS is released from caveolin-1 and translocates to the cytosol, where it dimerizes, binds its substrate L-arginine, and releases NO and L-citrulline. The cycle is completed by the eventual return of eNOS to the cell membrane as inactive enzyme (Fleming and Busse, 1999).

Recently, a novel Ca^{2+}/calmodulin-independent mechanism for eNOS activation has been described in mammalian endothelial cells (Igarashi et al., 1999). Exogenously administrated ceramide can activate eNOS in a Ca^{2+}-independent way. Thus, it was proposed that compounds able to activate the synthesis of ceramide might be regulators of eNOS activity.

Basic fibroblast growth factor (bFGF) is a powerful mitogen for most cell types, including Chinese hamster ovary fibroblasts (CHO-K1), and MAP kinase cascade has been demonstrated to represent a major transduction mechanism for this growth factor-induced cell proliferation. CHO-K1 cell duplication dramatically decreases if this enzymatic cascade is blocked, inhibiting MEK activity (Florio et al., 1999a). Through the regulation of endothelial cell proliferation and migration, bFGF represents also one of the major angiogenic factors produced by different types of tumors including most of human glioblastomas (Schmidt et al., 1999). Angiogenesis is now regarded as one of the most important tumor-mediated events responsible for tumor growth and dissemination (Folkman, 1995). NO production represents one of the main intracellular mechanisms responsible for tumor-dependent neoangiogenesis (Ziche et al., 1997). It has been demonstrated that NO, among its numerous intracellular functions, can stimulate cell proliferation in endothelial (Ziche et al., 1997) but also in CHO-K1 cells (Cordelier et al., 1997), mainly through the activation of the cGMP/protein kinase G (PKG) pathway (Cordelier et al., 1997). Although the role of NO in the activity of many angiogenic factors, such as vascular endothelial growth factor, is well defined (Ziche et al., 1997), the capability of bFGF to induce this intracellular second messenger is still controversial.

The aim of this study was to evaluate whether bFGF is able to activate the eNOS and to study the cellular and molecular mechanisms that mediate such an effect. Moreover, we studied the correlation between NO production induced by bFGF and its proliferative activity in CHO-K1 cells.

Materials and Methods

Materials

The following reagents were purchased as indicated: *N*-(1-naphthyl)ethylene diamide, sulfanilamide, and sodium nitroprusside (Sigma, St. Louis, MO); tricyclo-decan-9-yl xanthate (D609), Ly-83583, 8-bromo-cGMP, BAPTA/AM, KT 5823, *S*-methyl-isothiourea sulfate, L-N^5-(1-iminoethyl)-ornithine dihydrochloride (L-NIO), cholecystokinin (CCK), N^{ω}-NO_2-L-arginine (NNA), and N^G-nitro-L-arginine methyl ester hydrochloride (L-NAME) (Calbiochem, San Diego, CA); *N*-acetyl D-*erythro*-sphingosine, dihydro-*N*-acetyl D-*erythro*-sphingosine, *N*,*N*-dimethyl-sphingosine, fumonisin B1, and U 73122 (Alexis, Läufelfingen, Switzerland); [*methyl*-^{3}H]thymidine and L-[^{3}H]arginine (Amersham Biosciences, Piscataway, NJ); vanadate (ICN, Costa Mesa, CA); and sodium pyrophosphate (Merck, Whitehouse Station, NJ).

Antibodies

Anti-eNOS, -nNOS, -iNOS, and anti-caveolin 1 were from Santa Cruz Biotechnology (Santa Cruz, CA); anti-ERK1/2, phospho-ERK1/2, anti-phospho(Ser^{1179})-eNOS, anti-AKT, and phospho(Ser^{473})-AKT were from New England Biolabs (Beverley, MA)

Cell Culture

CHO-K1 were cultured under sterile conditions in Ham's F-12 medium (Invitrogen, Carlsbad ,CA) supplemented with 10% fetal calf serum (Invitrogen). Primary cultures of human skin fibroblasts from healthy subjects were obtained as described previously (Thellung et al., 1999). Fibroblasts from patients with Niemann-Pick disease were obtained from the "Laboratorio di Diagnosi PrePostnatale Malattie Metaboliche" (Istituto G. Gaslini, Genova Italy) using specimens from the collection "Cell lines and DNA bank from patients affected by genetic diseases". Three independent preparations

were used. Both fibroblasts cultures were performed in Dulbecco's modified Eagle's medium supplemented with 10% fetal calf serum (Invitrogen). Pertussis toxin (180 ng/ml) treatment was performed in serum-free medium for 18 h before the experimental treatments.

Determination of NO Production

Determination of Nitrite Accumulation Based on the Griess Reaction. NO, produced from the conversion of L-arginine to L-citrulline, is mainly oxidized to nitrite, which is an indicator of NO synthesis.

Nitrite concentration was measured using the Griess reaction in a colorimetric assay. Briefly, a solution containing 1% sulfanilamide and 0.1% *N*-(1-naphthyl)ethylene diamide in 2.5% H_3PO_4 is mixed with the cell culture medium (1:1) to form a purple azo-dye. Cells were plated in 24-well plates at a density of 1×10^5/well; after 24 h, they were treated with the test compounds for the indicated times. At the end of the incubation, the cell culture medium was added to the Griess reagent (1:1), and the optical density (absorbance) was measured at 550 nm after 10 min.

Determination of the L-[^{3}H]Citrulline Accumulation. The conversion of L-arginine in L-citrulline was monitored by measuring the production of L-[^{3}H]citrulline after incubation of the extract cytosolic fraction with L-[^{3}H]arginine, using the Stratagene kit (Stratagene, La Jolla, CA), following the manufacturer's instructions. Briefly, cells were mechanically homogenized in a buffer containing 24 mM Tris-HCl, pH 7.4, 1 mM EDTA, and 1 mM EGTA, the particulate fraction was pelleted (14,000*g*, 5 min), and the cytosolic fraction was collected and incubated (10 mg/ml) in a reaction buffer (25 mM Tris HCl, pH 7.4, 1 μM flavin adenine dinucleotide, 1 μM flavin adenine mononucleotide, and 3 μM tetrahydrobiopterin) to which 1.2 mM NAPDH, 0.25 μCi of L-[^{3}H]arginine, and 750 μM $CaCl_2$ have been added. The reaction was carried out for 60 min and then stopped with 400 μl of 50 mM HEPES, pH 5.5, and 5 mM EDTA. The formed [^{3}H]citrulline, derived from the NO production, was then recovered by chromatography and measured in a β-counter.

[^{3}H]Thymidine Incorporation Assay

DNA synthesis was quantified using the [^{3}H]thymidine incorporation assay. Cells were seeded into 24-multiwell plates at a density of 5×10^5/well. After 24 h, cells were serum-deprived for 24 h and then treated with the test substances for 16 h. In the last 4 h of treatment, cells were pulsed with 1 μCi/ml of [^{3}H]thymidine. Cells were collected by trypsin treatment for 5 min at 37°C and then filtered under vacuum through glass-fiber filters (GF/A; Whatman, Clifton, NJ). Unincorporated labeled nucleotides were removed by sequential 10 and 5% trichloroacetic acid (Sigma) and 95% ethanol washes. The filters containing the trichloroacetic acid-insoluble fraction were measured for radioactivity in a scintillation counter.

Immunofluorescence

The subcellular localization of eNOS and caveolin 1 was evaluated by indirect immunofluorescence experiments. Cells, plated on glass cover slips, were fixed in 4% paraformaldehyde for 15 min. After three washes in PBS, cells were permeabilized with 0.1% Triton X-100 for 5 min, washed again with PBS, and treated with PBS-glycine (1 M) for 10 min. Cells were stained with the primary antibody in PBS/0.1% FBS for 1 h, washed again three times with PBS, and then incubated with anti-rabbit fluorescein isothiocyanate-conjugated or anti-rabbit rhodamine-conjugated secondary antibody (Jackson ImmunoResearch Laboratories, West Grove, PA) (1:200) for 20 min. After washing in PBS and deionized H_2O, coverslips were mounted using Moviol (Calbiochem) and analyzed on a confocal microscope (argon laser excitation at 468 and 580 nm; 60× objective, MRC 1000; Bio-Rad, Hercules, CA) with a 0.4-μm step in z-plane acquisition. Each experiment was performed at least three times in duplicate.

Immunoprecipitation and Western Blot

CHO-K1 cells were plated in 10-cm Petri dishes until they reached 75% confluence. Then they were treated for the specified times with the test reagents. After two washes in PBS, cells were harvested in ice-cold lysis buffer containing 100 nM Tris-HCl, pH 8, 150 mM NaCl, 1% Nonidet P40, 0.4 mM EDTA, 10 mM NaF, 2 mM vanadate, 10 mM sodium pyrophosphate, 0.1 mg/ml phenylmethylsulfonyl fluoride, and a protease inhibitor mix (Complete; Roche Diagnostics, Mannheim, Germany). Soluble proteins (500 μg/ml) were incubated for 2 h at 4°C with anti-caveolin 1 antibody (1 μg/mg of protein) with continuous rotation. The samples were then incubated for 1 h at 4°C, with continuous rotation, with 50 μl of Sepharose-protein A (Sigma) to pellet the immunocomplexes. After three washes in the same lysis buffer, the immunoprecipitated proteins were resolved through a 10 or 15% SDS-polyacrylamide gel, transferred to a polyvinylidene difluoride membrane (Bio-Rad), and probed with the primary antibody. Immunoreactive proteins were visualized by the enhanced chemiluminescence immunodetection system (Amersham Biosciences).

Intracellular Calcium Measurement

Cells were plated on 25-mm glass coverslips and transferred to 35-mm Petri dishes. After 24 h, cells were serum-starved for a further 24 h. On the day of the experiment, cells were washed for 10 min with a balanced salt solution (HEPES 10 mM, pH 7.4, 150 mM NaCl, 5.5 mM KCl; 1.5 mM $CaCl_2$, 1.2 mM $MgSO_4$, and 10 mM glucose). Then cells were loaded with 4 μM Fura-2 penta-acetoxymethyl ester (Calbiochem) for 20 min at room temperature. Fluorescence measurements were performed as reported previously (Florio et al., 1999b). Briefly, Fura-2 fluorescence was imaged with an inverted Nikon diaphot microscope using a Nikon 40×/1.3 numerical aperture Fluor DL objective lens. Fluorescence (ratio 340/380) was then evaluated and converted in $[Ca^{2+}]_i$ using the Quanticell apparatus (VisiTech, Sunderland, UK). For the calibration of fluorescence signals, we used cells loaded with Fura-2; R_{max} and R_{min} are ratios at saturating and zero $[Ca^{2+}]_i$, respectively, and were obtained by perfusing the cells with a salt solution containing 10 mM $CaCl_2$, 2.5 μM digitonin, and 2 μM ionomycin and subsequently with a Ca^{2+}-free salt solution containing 10 mM EGTA. The values of obtained R_{max} and R_{min} were used to calculate the $[Ca^{2+}]_i$ using the Quanticell software, according to the equation of Grynkiewicz et al. (1985).

cGMP Detection

cGMP levels were measured in cell extract from confluent cells seeded in six multiwell plates and treated for the indicated times with the test substances in the presence of 500 μM IBMX as phosphodiesterase inhibitor. Cells were then extracted for 24 h at 4°C with 99% ethanol/1% HCl (v/v), and the supernatant was collected for the quantification of the cGMP by high-performance liquid chromatography (HPLC). Before the analysis, the samples were centrifuged and filtered through a nylon-66 filter, 0.2 μm (Rainin Instrument, Woburn, MA). The clear filtrate obtained was used directly for HPLC assay, as described previously (Spoto et al., 1991), or stored at −80°C until the assay.

Chromatographic Apparatus. The HPLC system (Beckman Coulter, Fullerton, CA) consisted of a two 110A pumps, a variable wavelength spectrophotometer (Spectroflow 783; Kratos Analytical) measuring at 254 nm; and an autosampler Promis (Spark Holland, Emmen, the Netherlands).

Chromatographic Conditions. The column used was a 5-μm Li-Chrospher 100CH 18/2 (250 × 4 mm) (Merck). The mobile phase employed for the separation of nucleotides consisted in 200 mM ammonium acetate, pH 6.0, with 2% acetonitrile (v/v). The flow rate was 1 ml/min; the detection was performed at 254 nm. Peak identities were confirmed by coelution with standards. Quantitative measurements were carried out by comparison using standard solutions of known concentrations.

Ceramide Measurement

After appropriate treatments, cells were washed in PBS and then harvested by scraping in 3 volumes of lysis buffer (0.5 M sucrose, 20 mM Tris HCl, pH 6.8, 150 mM NaCl, 3 mg/ml leupeptin, 0.5 mM phenylmethylsulfonyl fluoride, and 0.5 mM dithiothreitol) and normalized for protein content using the the Bradford method (Bradford, 1976). After sonication, total lipid content was extracted for 1 h in chloroform/methanol (2:1, v/v) containing butylated hydroxyanisole as antioxidant (Folch et al., 1957). After a brief centrifugation, the lower phase was collected, dried under nitrogen stream, and stored at −80°C until the assay. Samples were then processed for basic hydrolysis to remove other lipid species, dissolved in dimethyl sulfoxide, and then analyzed by high-performance liquid chromatography–electrospray ionization-mass spectrometry, as reported previously (Kalhorn and Zager, 1999) with modifications. We used a Hewlett Packard 1090 series II liquid chromatography system directly coupled with a Hewlett Packard 5989A "Engine" single-quadrupole mass spectrometer. An Alltech Adsorbosphere XL C8 300A 5μ column (250 × 4.6 mm) was used and an isocratic mobile phase of 20 mM methanol/acetic acid (90:10) at a flow rate of 0.8 ml/min was applied. The mass range was set to 100 to 800 atomic mass units, and the signal was optimized to observe the monosodium adduct of the molecular ion in the positive ion mode. The capillary exit voltage was adjusted to optimize the expected *m/z* ratio.

Statistics

Experiments involving NO and cGMP measurements or cell proliferation were performed in quadruplicate. All the experiments were repeated at least three times. Statistical analysis was performed by means of one-way analysis of variance; $p \leq 0.05$ was considered statistically significant.

Results

bFGF Effects on NO Production in CHO-K1 Cells. bFGF treatment (30 ng/ml) of CHO-K1 cells caused time-dependent increases in production of both NO (measured using the Griess reagent) and cGMP (assessed by HPLC experiments) that were detectable starting after 1 h of stimulation and then followed by a constant increase for longer treatments, with a maximum after 24 h (data not shown). To maximize the cell response to bFGF, all the subsequent experiments were performed after 24 h of treatment. In Fig. 1A, the effect of different bFGF concentrations on NO production is shown. bFGF, dose dependently induced NO production starting at the concentration of 5 ng/ml. The increase in NO, in turn, activated a soluble guanylyl cyclase to stimulate cGMP production, the intracellular concentration of which was indeed significantly increased (by about 300%) (Fig. 1B). Similar results were also obtained by measuring the NO production as conversion of L-[^{3}H]arginine in L-[^{3}H]citrulline (basal, 19,734 ± 425 cpm/well; bFGF, 33,446 ± 759 cpm/well; $p < 0.01$). It was reported previously that at least two isoforms of NOS are expressed in CHO-K1 cells (i.e., nNOS and eNOS) (Cordelier et al., 1999). We confirmed these data by reverse transcription-polymerase chain reaction (data not shown) and Western blot analysis, which identified both

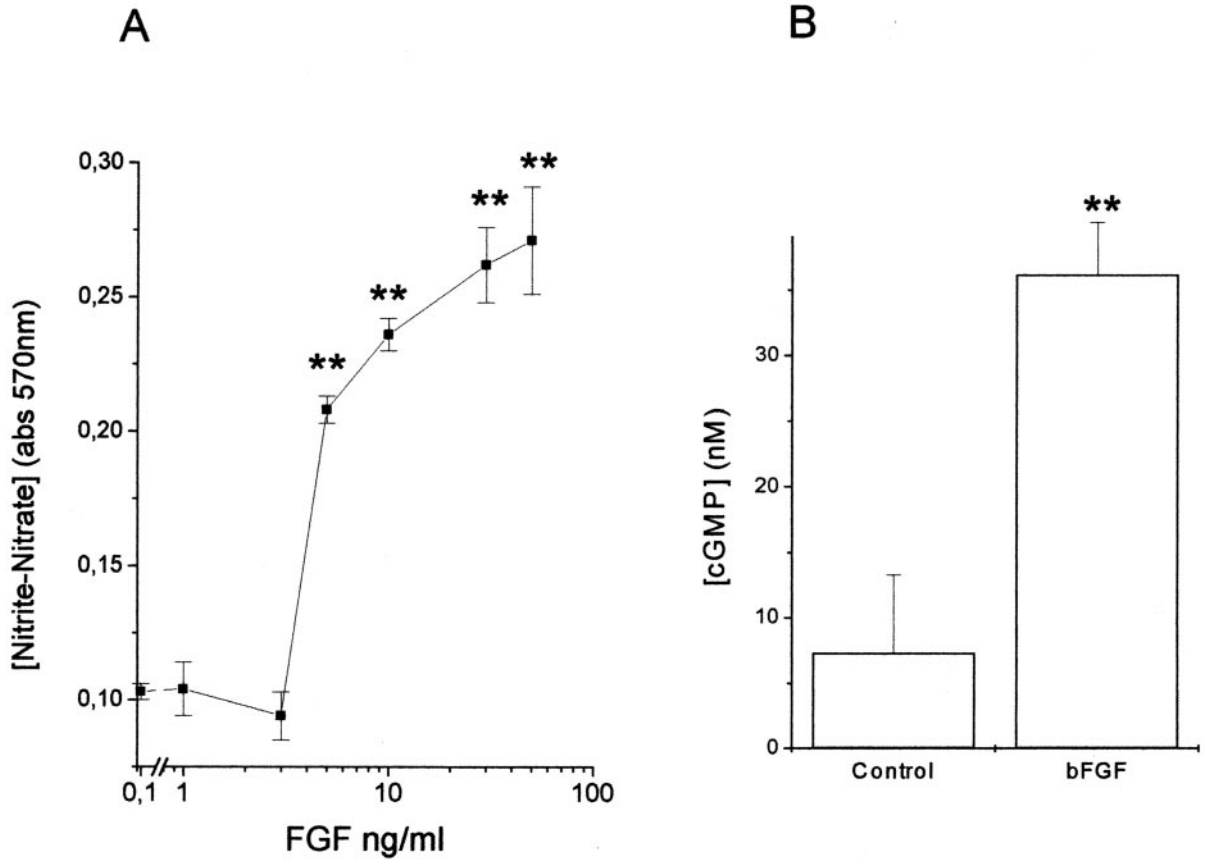

Fig. 1. A, dose-response of bFGF on NO production evaluated with the Griess reaction. Cells were treated for 24 h with bFGF (1–100 ng/ml). Data are expressed as nitrate/nitrite accumulation measured as optical density (absorbance at 570 nm). B, bFGF (30 ng/ml, for 24 h) induced cGMP accumulation, measured in HPLC experiments, in the presence of the the phosphodiesterase inhibitor IBMX. **, $p < 0.01$ versus respective basal values

cNOS isoforms in these cells (Fig. 2A). Conversely, iNOS was detected under neither basal nor bFGF-stimulated conditions (Fig. 2A). These data were also confirmed using a pharmacological approach. *S*-Methyl-isothiourea, a rather selective iNOS inhibitor (Szabo et al., 1994), reduced bFGF-dependent NO production only slightly, whereas the L-NIO compound that affects eNOS with higher affinity than the other NOS isoforms (Rees et al., 1990) reduced the NO production to a level similar to that obtained with the powerful but nonspecific NOS inhibitors L-NAME and NNA (Rees et al., 1990) (Fig. 2B). These results suggest that bFGF may induce NO synthesis through the activation of eNOS.

bFGF Activation of eNOS Is Ca^{2+}-Independent. Both cNOS isoforms have been reported to be activated in a Ca^{2+}-dependent manner. Thus we tested whether, in CHO-K1 cells, bFGF-induced NO production was the result of an increase in $[Ca^{2+}]_i$. We pretreated the cells with increasing concentrations (3–100 μM) of the cell-permeable Ca^{2+} chelator BAPTA-AM and tested, under these experimental conditions, the effects of bFGF on NO production. However, bFGF (30 ng/ml), in the presence of the highest BAPTA-AM concentration, was still able to induce NO synthesis to levels comparable with those observed in control cells (Fig. 3A). As an internal control, we evaluated the effects of CCK, a peptide known to activate the NOS in a Ca^{2+}-dependent manner through the activation of the CCK-A receptor subtypes, which are expressed in the CHO-K1 cells (Cordelier et al., 1999). CCK (1 μM) induced a significant increase in NO production that was completely blocked by the pretreatment with BAPTA-AM (Fig. 3A). Moreover, in microfluorometric experiments, we demonstrated that bFGF treatment does not modify $[Ca^{2+}]_i$ even at the high concentrations (100 ng/ml) that occur when treating the cells with CCK (1 μM) (Fig. 3B). To identify the possible intracellular mechanisms involved in bFGF effects, we tried to inhibit the NO production induced by this growth factor by blocking different signal transduction pathways known to be activated by FGF receptors. However, all the compounds that we tested [the inhibitors of MEK, phosphatidyl inositol-3 kinase, phospholipase C (PLC), and protein kinase C: PD98059, wortmannin, U73122, and staurosporine, respectively] did not affect the NO production caused by 30 ng/ml bFGF (data not shown).

bFGF Activation of eNOS Is Mediated by a Sphingomyelinase-Dependent Ceramide Production. Recently, a Ca^{2+}-independent regulation of NO production by eNOS was identified that is mediated by exogenously administered ceramide in endothelial cells (Igarashi et al., 1999).

Also, in CHO-K1 cells, the cell permeable C2:0 (Fig. 4) and C8:0 ceramide species (data not shown) caused significant and dose-dependent (10–40 μM) increases in NO synthesis. This effect was specific because dihydroceramide, an inactive immediate precursor to ceramide, was completely ineffective (Fig. 4). To demonstrate that ceramide may represent a novel second messenger induced by bFGF, we analyzed whether inhibitors of the enzymes responsible for ceramide synthesis could revert the bFGF-dependent NO generation. Ceramide may be synthesized through two different intracellular pathways: the hydrolysis of sphingomyelin to ceramide, operated by a family of sphingomyelinases, or the conversion of sphingosine in ceramide through the activity of a ceramide synthase (Hannun, 1996). The first pathway is affected by the compound D609 via the inhibition of a phosphatidyl choline-specific PLC (Cifone et al., 1995) and by desipramine, a more specific inhibitor for the acidic sphingomyelinase isoform (Albouz et al., 1983), whereas the latter is blocked by fumonisins (Wang et al., 1991). In CHO-K1 cells, D609 and desipramine

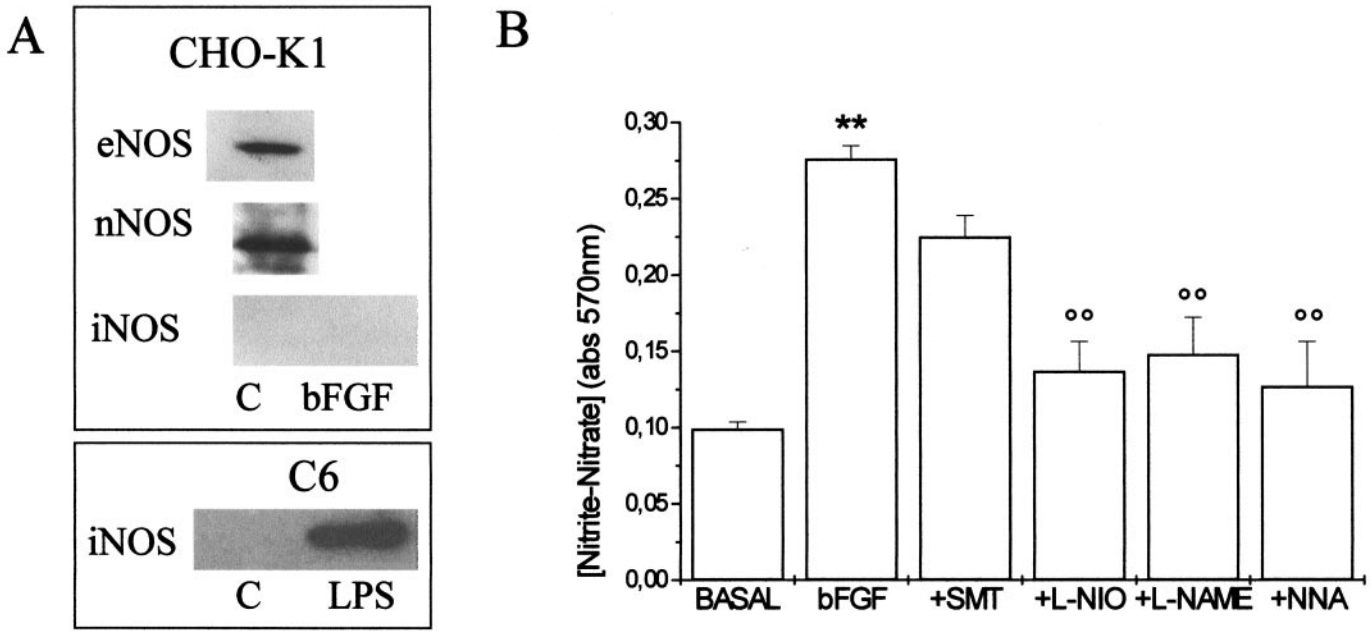

Fig. 2. A, Western blot analysis showing the expression of eNOS and nNOS in CHO-K1 cells. The inducible isoform of the enzyme is not detectable in these cells under either basal or bFGF-stimulated conditions. C6 glioma cells after LPS stimulation (10 μg/ml, 6 h) were used as a positive control for iNOS expression. The apparent molecular masses of the bands shown are: 140 kDa for eNOS, 160 kDa for nNOS, and 130 kDa for iNOS. B, the effect of nitric oxide synthase inhibitors, selective for different isoforms of the enzyme, on bFGF-induced NO production. Cells were stimulated with bFGF (30 ng/ml, 24 h) in the absence or presence of *S*-methyl isothiourea sulfate (SMT; a selective inhibitor of iNOS), L-NIO (which affects eNOS with higher affinity), and the nonspecific NOS inhibitors NNA and L-NAME. Data are expressed as nitrate/nitrite accumulation measured as optical density (absorbance at 570 nm). **, $p < 0.01$ versus the basal value; °°, $p < 0.01$ versus bFGF-stimulated value

almost completely abolished bFGF-dependent NO synthesis, whereas fumonisin B1 was totally ineffective (Fig. 5B). Moreover, the preincubation with D609 dose-dependently reduced the cGMP production induced by bFGF (Fig. 5C), confirming that bFGF may regulate the NO/cGMP production through the modulation of the sphingomyelinase activity. Conversely, no effects of desipramine were observed on CCK-stimulated NO synthesis (data not shown). These results were confirmed by the exogenous administration of a recombinant acidic sphingomyelinase that dose-dependently activated the NO synthesis (30 and 300 mU/ml = +50 and +110%, respectively, versus basal NO production).

The role of sphingomyelinase in bFGF signalling was further demonstrated by analyzing the effects of this growth factor on cultures of fibroblasts derived from patients with Niemann-Pick disease, who are genetically deficient in sphingomyelinase. As a control, we compared the results obtained from these cells with primary cultures of fibroblasts derived from healthy subjects and with CHO-K1 cells. In agreement with previous studies (Koeck and Kremser, 2001), we found that primary cultures of human fibroblasts, derived from both healthy subjects and patients with Niemann-Pick disease, express eNOS (Fig. 5A). Conversely, similarly to CHO-K1 cells, bFGF treatment did not induce iNOS expression and activity in either culture (data not shown).

Similarly to CHO-K1 cells, bFGF induced the synthesis of high concentrations of NO in human normal fibroblast cultures in a D609- and desipramine-sensitive manner (Fig. 5B). Conversely, bFGF treatment was completely ineffective in Niemann-Pick cells (Fig. 5B), although a significant increase in NO synthesis was induced in all the fibroblast cultures (Niemann-Pick cells included) by the treatment with CCK (data not shown), which activates NOS through a Ca^{2+}-

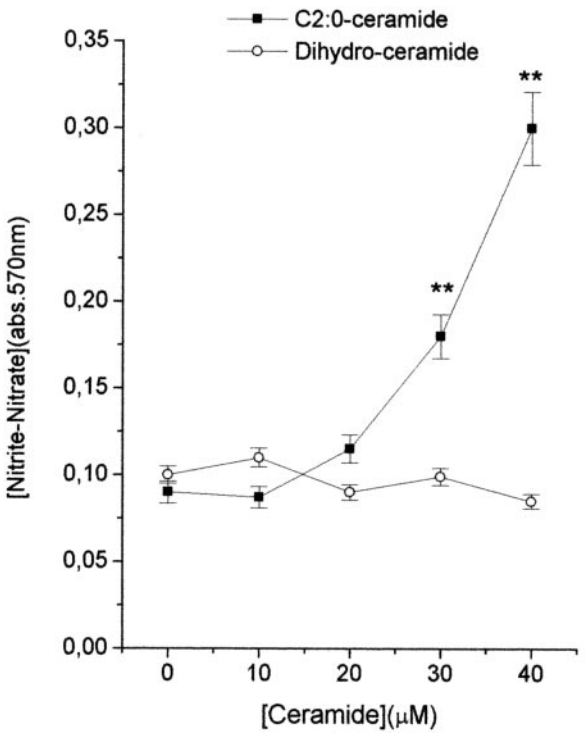

Fig. 4. Effect of increasing concentrations (10–40 μM, 3 h) of the cell-permeable C2:0 ceramide and its inactive immediate precursor dihydroceramide on NO synthesis. Data are expressed as nitrate/nitrite accumulation measured as optical density (absorbance at 570 nm). **, $p < 0.01$ versus the basal value

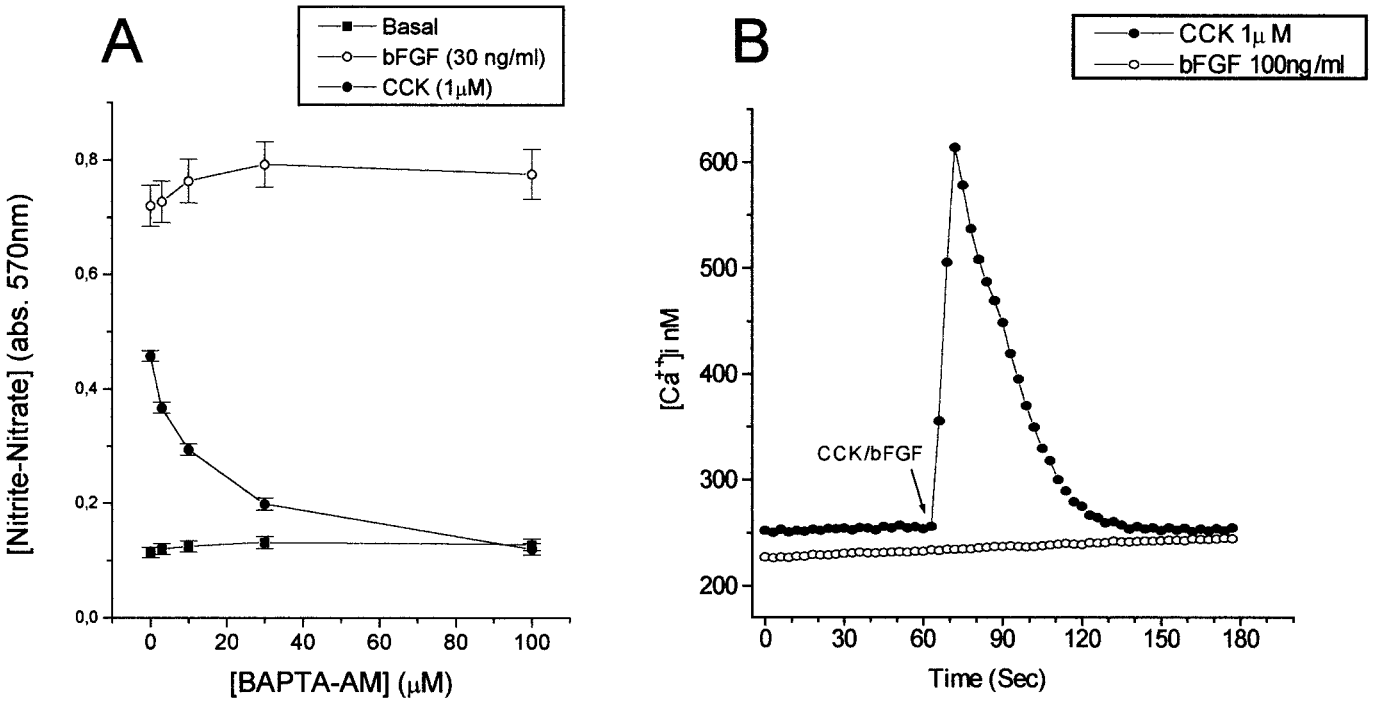

Fig. 3. A, effect of increasing concentrations of the cell permeable intracellular Ca^{2+} chelator, BAPTA-AM, on basal, CCK-, and bFGF-induced NO production. Data are expressed as nitrate/nitrite accumulation measured as optical density (absorbance at 570 nm). B, effects of bFGF and CCK on the intracellular calcium concentration in CHO-K1 cells, measured using the fluorescent probe Fura 2, in microfluorometry. At least 15 cells per field were analyzed, and the data are expressed as mean values.

dependent mechanism (see Fig. 3). Moreover, we were able to overcome the Niemann-Pick cell phenotype by exogenous administration of either C2:0 (data not shown) or C8:0 (Fig. 5D) ceramide species, which induced NO production, bypassing the lack of sphingomyelinase activity. Again, no effects were observed in Niemann-Pick fibroblasts using the inactive ceramide precursor dihydroceramide (Fig. 5D)

To directly demonstrate that FGF receptors activation causes the synthesis of ceramide, we measured the concentration of different ceramide species in control and bFGF-treated cells, using the HPLC–electrospray ionization-mass spectrometry technique, as reported previously (Kalhorn and Zager, 1999), with modifications (see *Materials and Methods*). In these experiments, bFGF (30 ng/ml) treatment caused a significant increase in the intracellular ceramide content. The extracted ion chromatogram of the lipid content of bFGF-treated CHO-K1 cells is shown in the Fig. 6C. In particular, a peak at *m/z* 532.6, $[M\text{-}H+Na]^+$, characteristic of C14:0 ceramide species (see Fig. 6A), was detected, whereas it was completely absent in the untreated cells (Fig. 6B). Moreover, other smaller peaks were also detected in bFGF-treated cells, corresponding to C16:0 and C6:0 ceramide isoforms (Fig. 6C).

bFGF Induces a Cytosolic Translocation of eNOS in a Ceramide-Dependent Manner. To delve deeper into the characterization of the mechanisms by which bFGF regulates the production of NO, we analyzed the effect of bFGF treatment on the intracellular localization of eNOS. Indeed, the inactive form of this enzyme is bound to the membrane in caveolae but, upon activation, it translocates to the cytosol (Fleming and Busse, 1999). By means of indirect immunofluorescence and confocal microscopy analysis, we found that, in basal conditions, most of the eNOS was localized in the membrane with a characteristic distribution in patches, probably corresponding to the caveolae (Fig. 7, top center). Indeed, using an antibody directed against caveolin 1, the major protein constituting the caveolae, we obtained a simi-

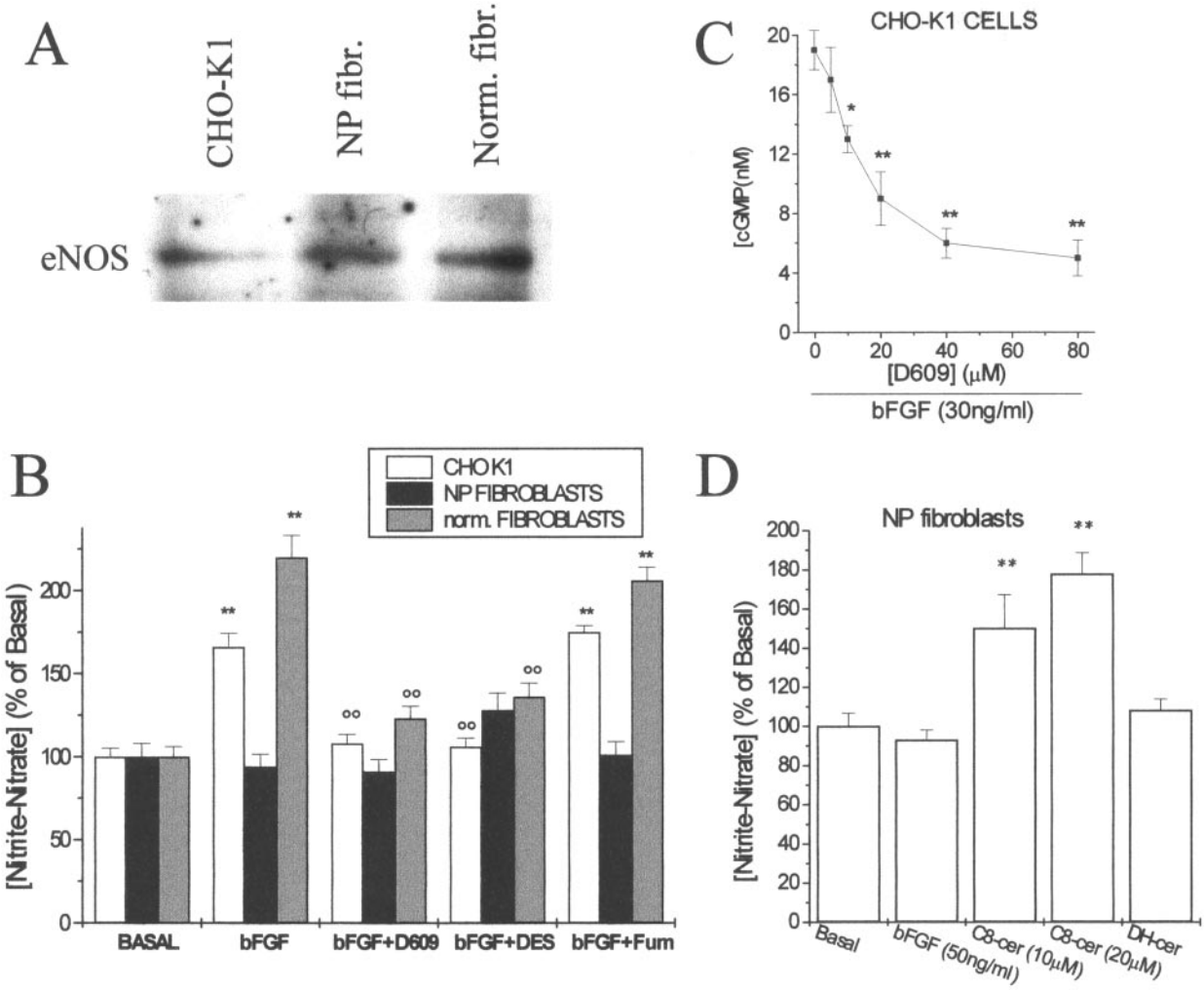

Fig. 5. A, Western blot analysis of the expression of eNOS in primary cultures of human skin fibroblasts derived from patients with Niemann-Pick disease (NP) or healthy subjects (norm), in comparison with the expression in CHO-K1 cells. All the fibroblast cultures analyzed express a significant amount of eNOS protein. The apparent molecular mass of the bands shown is 140 kDa. B, effect of inhibitors of ceramide production D609 (20 μM), desipramine (50 μM), or fumonisin B1 (40 μM), on bFGF (30 ng/ml)-induced NO synthesis in CHO-K1 cells and primary cultures of human skin fibroblasts derived from patients with Niemann-Pick disease (NP) or healthy subjects (norm). Data are expressed as a percentage of the basal nitrate/nitrite accumulation measured as optical density (absorbance at 570 nm). **, $p < 0.01$ versus respective basal value; °°, $p < 0.01$ versus respective bFGF-stimulated values. C, effect of D609 (20 μM) of bFGF (30 ng/ml)-induced cGMP synthesis in CHO-K1 cells, measured in HPLC experiments, in the presence of the phosphodiesterase inhibitor IBMX. *, $p < 0.05$ versus bFGF value. D, effect of bFGF (30 ng/ml), C8:0 ceramide (10 and 20 μM) and dihydroceramide (DH-cer) (20 μM) on fibroblasts derived from patients with Niemann-Pick disease (NP). Data are expressed as a percentage of the basal nitrate/nitrite accumulation measured as optical density (absorbance at 570 nm). **, $p < 0.01$ versus basal value.

lar localization pattern of the fluorescence signal (Fig. 7, top left). After merging the fluorescence signals, a clear colocalization of the two proteins was observed (Fig. 7, top right). In bFGF-stimulated cells, eNOS localization showed a much more diffuse signal, mainly in the cytosol and around the nucleus, indicating that the enzyme was released from the caveolae, and translocated to the cytosol in the active form (Fig. 7, bottom center). Indeed, in the bFGF-stimulated conditions, the colocalization between eNOS and caveolin 1 was no longer observed (Fig. 7, bottom right). Conversely, no significant changes in nNOS intracellular localization were observed (data not shown). The blockade of the sphingomyelinase activity obtained using the compound D609 (20 μM) caused a significant decrease in the bFGF-induced translocation of eNOS, showing an immunofluorescence image very similar to that of the control cells (data not shown), confirming that the eNOS activation by bFGF was dependent on the ceramide production. A further analysis of the role of eNOS in the NO production induced by bFGF was performed by evaluating in Western blots the level of eNOS after immunoprecipitation with antibodies directed against caveolin 1, as reported previously (Feron et al., 1996). bFGF and C2:0 ceramide treatments significantly reduced the amount of eNOS bound to caveolin 1 (Fig. 8). Moreover, the pretreatment with

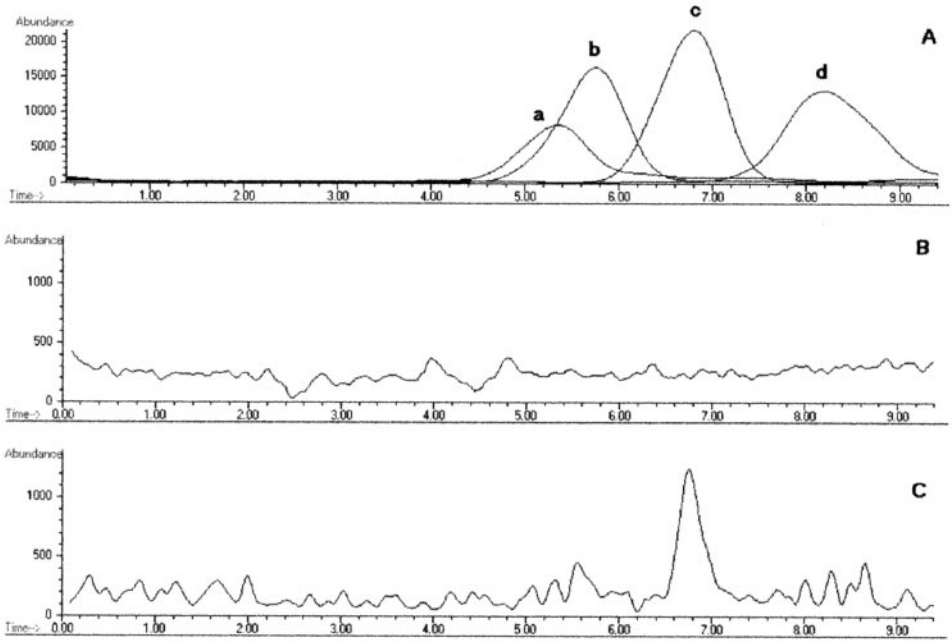

Fig. 6. Extracted ion chromatograms of molecular ion (monosodium adducts) from ceramide standards (A), control cells (B), and 30 ng/ml bFGF-treated cells (C). Ceramide standards used in A are: a, C6:0 = *m/z* 420.6; b, C8:0 = *m/z* 448.6; c, C14:0 = *m/z* 532.6; d, C16:0 = *m/z* 560.8.

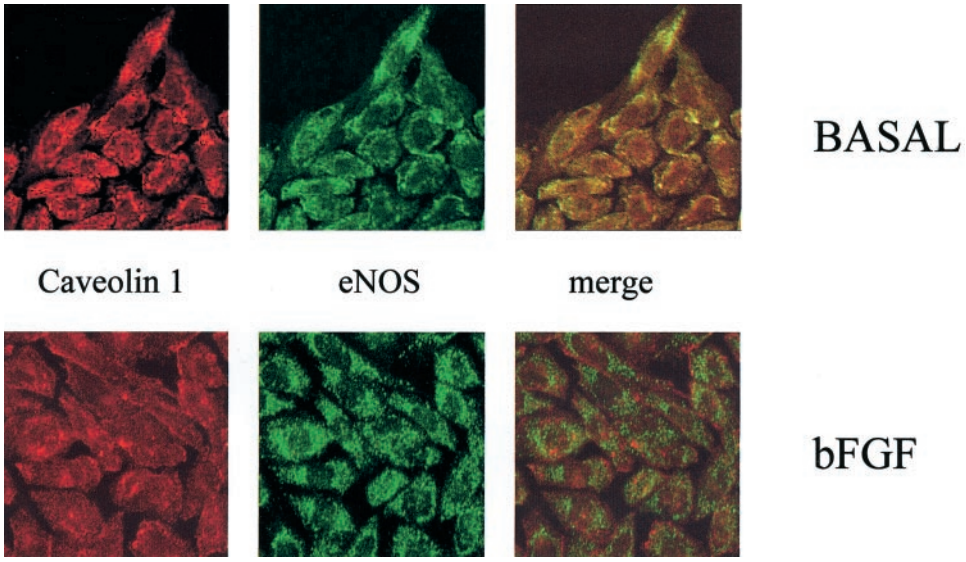

Fig. 7. Representative immunofluorescence pictures of eNOS localization in CHO-K1 cells using the specific antibodies directed against caveolin 1 (red) or eNOS (green). The merge of the two signals is also reported. Top, immunofluorescence signals in control cells; eNOS is almost completely anchored to the plasma membrane, showing a characteristic disposition in "patches". A fluorescence imagine comparable with what was observed using the eNOS antibody is also observed in control cells incubated with the anti-caveolin 1 antibody. The yellow color in the merge panel indicates the colocalization of the two proteins. Bottom, immunofluorescence signals in bFGF-treated cells. Membrane localization of eNOS is completely lost in cells treated for 1 h with bFGF (30 ng/ml), and the enzyme is spread in the cytosol, mainly in the perinuclear region. The absence of yellow in the merge panel indicates that dissociation between eNOS and caveolin 1 occurred. All the images were acquired using identical brightness parameters and contrast settings.

D609 caused a significant reduction in the bFGF effect (Fig. 8). As a control, we demonstrated that in all the samples, the same amount of caveolin 1 was immunoprecipitated (Fig. 8). Moreover, by comparing on Western blots and in densitometric analysis the amount of eNOS immunoprecipitated from 100 μg of total cell lysate using the anticaveolin 1 antibody and the amount of eNOS present in 100 μg of CHO-K1 lysate, we found that more than 70% of the total eNOS present in untreated cells was immunoprecipitated bound to caveolin 1(data not shown). These data confirm that the changes we observed after bFGF and ceramide treatments represent a quantitatively important protein-protein dissociation.

bFGF Activation of eNOS via Ceramide Production Does Not Involve Sphingosine 1-Phosphate Production. Besides its direct effects, ceramide may act through its metabolite sphingosine 1-phosphate (S1P), a biologically active sphingolipid that has been implicated in intra- and intercellular signaling via the activation of the EDG-1, EDG-3, and EDG-5 G-protein coupled receptors (Spiegel and Milstien, 2000). In particular, it was recently reported that the EDG-1 receptor activation by S1P may induce NO production via the Akt-dependent phosphorylation of eNOS (Ser^{1179}) (Igarashi et al., 2001). Thus, we evaluated whether ceramide, produced after bFGF treatment, may activate eNOS through its metabolism to S1P. We measured the increase in NO production induced by bFGF in the presence of the sphingosine kinase inhibitor *N*,*N*-dimethyl-sphingosine (DMS) (Edsall et al., 1998) to block the generation of S1P or, after pretreatment with pertussis toxin (PTX), to uncouple the EDG receptors from the G protein. However, neither treatment modified the bFGF effect (Fig. 9, A and B). Then we tested whether the phosphorylation of eNOS at Ser^{1179} by Akt was also relevant for the bFGF-dependent NO production. Western blot analysis using phospho-specific antibodies for both Akt and eNOS showed that bFGF treatment induced a slight and short-lasting phosphorylation of Akt (present after 2 min of treatment and completely abolished after 15 min) (Fig. 10A), whereas no effects were identified on eNOS phosphorylation after either 2 (data not shown) or 15 min of treatment (Fig. 10B), thus excluding the involvement of this pathway from the bFGF effects in CHO-K1 cells. Conversely, as internal control, we demonstrated that, in agreement with recent studies (Montagnani et al., 2001), insulin caused a more robust and long-lasting (still present after 15 min of treatment) activation (Ser^{473} phosphorylation) of Akt and eNOS phosphorylation (Fig. 10, A and B).

Role of NO Produced after bFGF Treatment in CHO-K1 Cell Proliferation. We investigated a possible

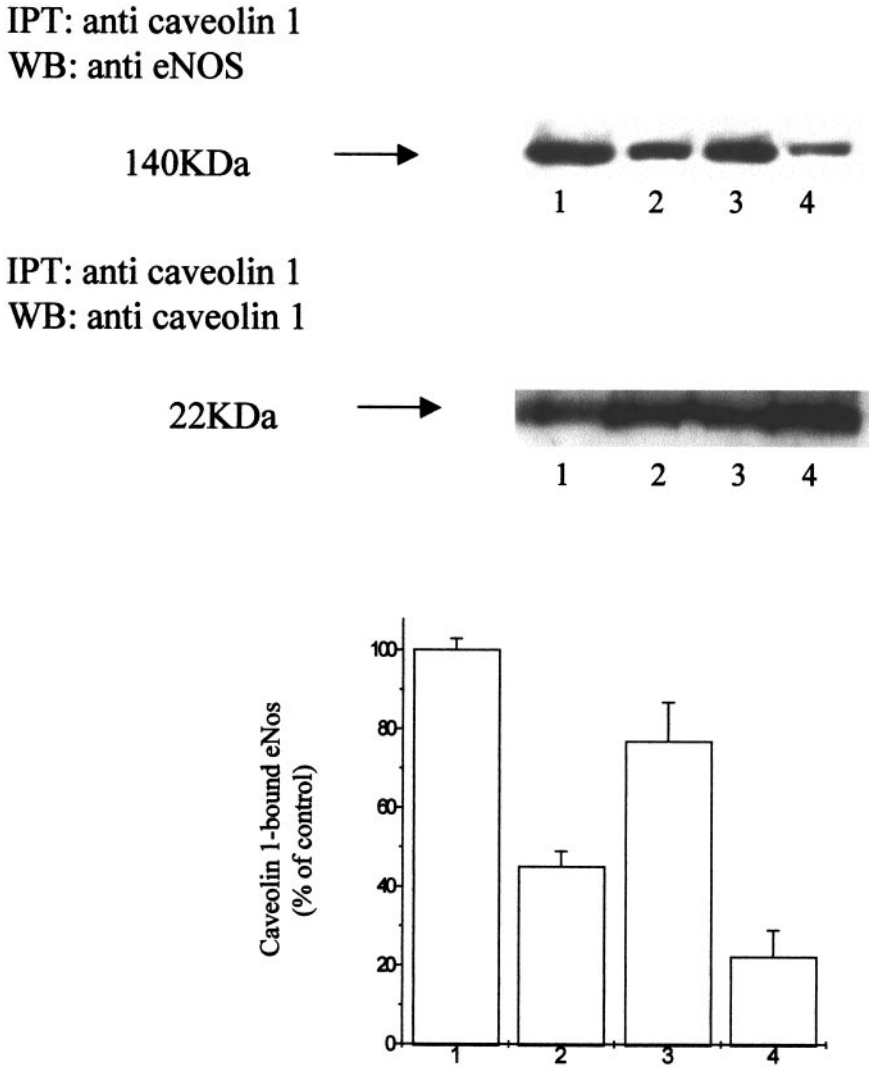

Fig. 8. Colocalization of eNOS and caveolin 1 in CHO-K1 cells. Cells were plated in 10-mm dishes and left untreated (lane 1) or treated for 1 h with bFGF (30 ng/ml) (lane 2), bFGF + D609 (20 μM) (lane 3), or C2:0 ceramide (20 μM) (lane 4). Equal amounts of proteins from total cell lysate (300 μg) were immunoprecipitated (IPT) with anti-caveolin 1 antibody. Western blot (WB) was performed using either anti-eNOS (top lanes) or anti-caveolin 1 (bottom lanes) antibodies, in two parallel gels. In the graph is reported the ratio of the densitometric analysis of the above depicted gels, expressed as 100% of the control cells. The experiments have been repeated three times with superimposable results.

physiological role for this novel signaling pathway activated by bFGF, involving the synthesis of ceramide, NO, and cGMP.

In CHO-K1 cells, treatment with sodium nitroprusside (SNP), a NO donor, caused a dose-dependent cell proliferation that was completely reversed by the guanylyl cyclase and PKG inhibitors Ly-83583 and KT 5823, respectively (Fig. 11A), indicating that, in these cells, the production of cGMP

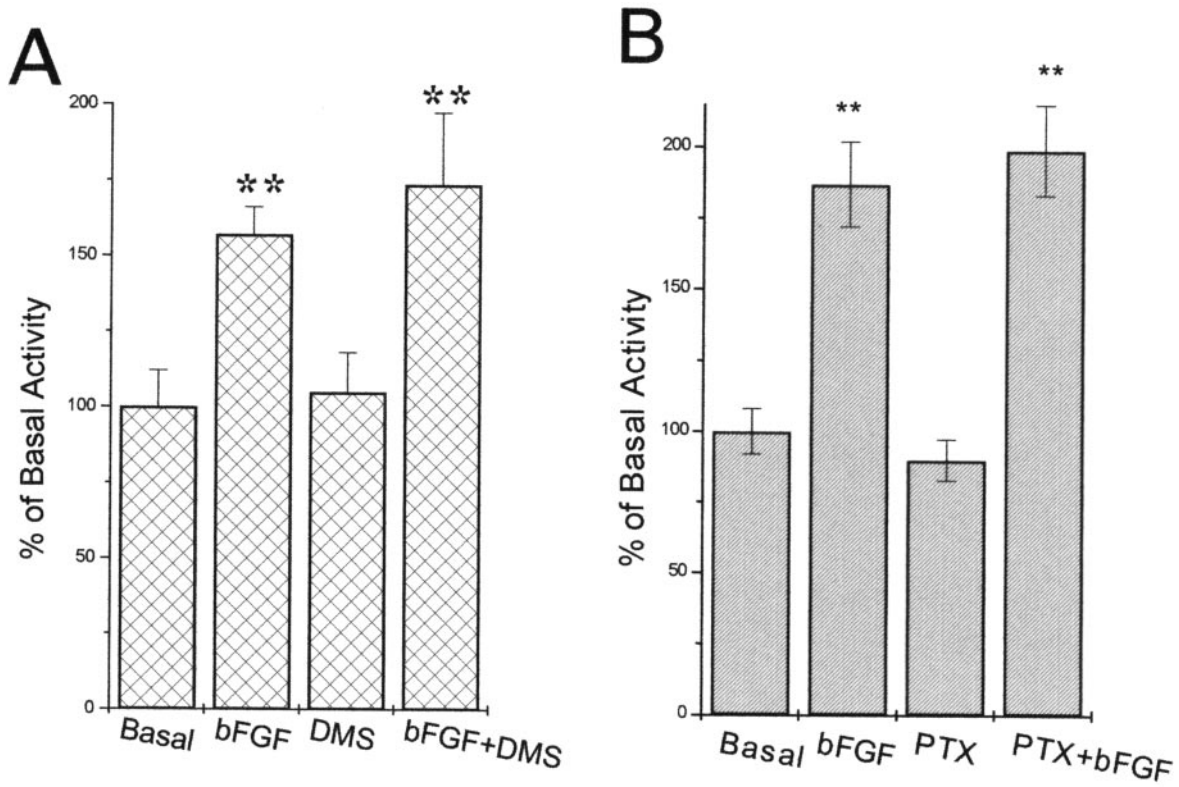

Fig. 9. Effect of the sphingosine kinase inhibitor DMS (A) and pertussis toxin (PTX) on bFGF-induced NO production. A, cells were treated with bFGF (30 ng/ml, 24 h) in the absence or presence of DMS; NO synthesis was evaluated by measuring the conversion of L-[^{3}H]arginine in L-[^{3}H]citrulline. B, cells were pretreated with PTX (200 ng/ml, 18 h), treated with bFGF (30 ng/ml, 24 h), and NO synthesis was evaluated by measuring the conversion of L-[^{3}H]arginine in L-[^{3}H]citrulline. Data are expressed as percentage of basal activity. **, $p < 0.01$ versus respective basal value

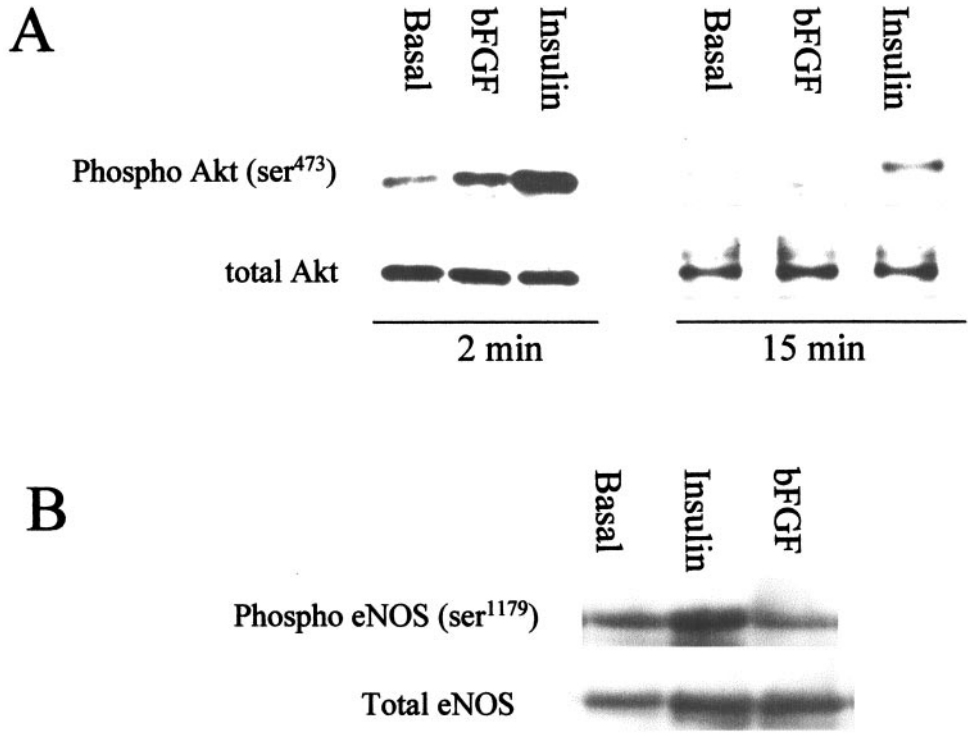

Fig. 10. A, effects of bFGF (30 ng/ml, 2 and 15 min) and insulin (170 nM, 2 and 15 min) on Akt activation, evaluated as Ser^{473}-phosphorylation in Western blot, using a phosphospecific antibody. Equal protein loading was demonstrated by probing the membrane with an antibody directed against the total Akt protein. B, effects of bFGF (30 ng/ml, 15 min) and insulin (170 nM, 15 min) on Ser^{1179}-phosphorylation of eNOS in Western blot, using a phosphospecific antibody. Equal protein loading was demonstrated by probing the membrane with an antibody directed against the total eNOS protein.

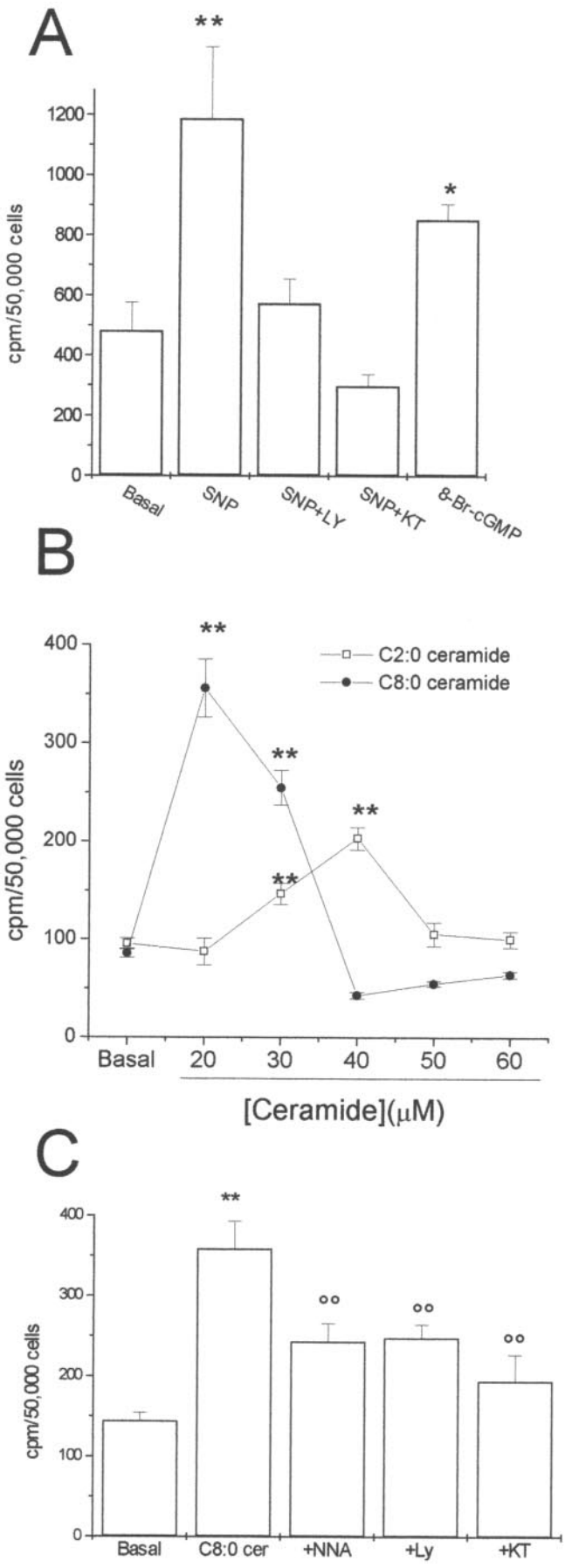

and the activation of PKG represent the final effectors of the NO synthesis as far as proliferative responses. This observation was further confirmed by testing the effect of the cell-permeable cGMP analog 8-bromo-cGMP, which significantly increased the DNA synthesis of the CHO-K1 cells (+77% versus untreated cells) (Fig. 11A). Under our experimental conditions, the treatment with C2:0 ceramide, representing the upstream activator of NO synthesis, also caused an increase in the cell proliferation. However, this effect was strictly dependent on the duration of the exposure and the concentration used, because ceramide is also a well-known inducer of apoptosis in many cell systems. We found that treatment for 18 h, even using low concentrations of C2:0 ceramide, caused dramatic cell death in the CHO-K1 cells (data not shown). However, if we exposed the cells to the C2:0 ceramide for 2 h and then replaced the medium with fresh serum-free medium up to 18 h, C2:0 ceramide (20–40 μM) was able to induce a significant increase in DNA synthesis (up to + 100%) (Fig. 11B). At higher concentrations, this effect was abolished (Fig. 11B); at 100 μM, a complete degeneration of the cells occurred after short treatment (data not shown). Similar results were obtained with the C8:0 ceramide. Similar to the C2:0 ceramide, the C8:0 ceramide caused a biphasic effect on CHO-K1 cell proliferation; it was proliferative at low concentrations and caused cell death at higher concentrations (Fig. 11B). However, compared with C2:0 ceramide, the dose-response curve of C8:0 ceramide was left-shifted with a maximal stimulatory effect at 20 μM (Fig. 11B). Interestingly, the pretreatment with NNA, Ly-83583, and KT5823 inhibitors of NOS, guanylyl cyclase, and PKG, respectively, caused a statistically significant inhibition of the ceramide-dependent proliferation (Fig. 11C), confirming that exogenous ceramide causes proliferation through the activation of the NO/cGMP system.

bFGF is a strong proliferative agent for CHO-K1 cells that acts mainly through the MAP kinase cascade and the activation of ERK1/2. To investigate whether the ceramide/NO/cGMP production induced by bFGF might also influence the proliferative response of this factor and interfere with the MAP kinase cascade, we tested the effects of the inhibitors of ceramide synthesis (D609), NOS (NNA), guanylyl cyclase (Ly-83583), and PKG (KT5823) on the CHO-K1 proliferation induced by bFGF. All these compounds, used at concentrations that do not affect the basal [^{3}H]thymidine uptake (20

Fig. 11. A, effect of the NO donor sodium nitroprusside (SNP; 1 μM) and 8-bromo-cGMP (1 μM) on CHO-K1 cell proliferation measured using the [^{3}H]thymidine incorporation assay. SNP effects were measured in the absence or presence of the guanylyl cyclase inhibitor Ly-83583 (LY; 10 nM) and the PKG inhibitor KT 5823 (KT; 100 nM). Cells (50,000/well) were serum-starved for 24 h and then treated for 18 h. In the last 4 h of treatment, cells were pulsed with 1 μCi/ml of [^{3}H]thymidine. Data are expressed as cpm/well. *, $p < 0.05$; **, $p < 0.01$ versus basal value. B, effect of increasing concentrations (20–60 μM) of C2:0 and C8:0 ceramide on CHO-K1 cell proliferation, measured using the [^{3}H]thymidine incorporation assay. C, effect of the NOS, guanylyl cyclase, and PKG inhibitors NNA, Ly-83583 (Ly), and KT 5823 (KT) on the C8:0-induced CHO-K1 cell proliferation, measured using the [^{3}H]thymidine incorporation assay. In B and C, cells (50,000/well) were serum-starved for 24 h and then received the appropriate treatments for 2 h. Then, the medium was removed and replaced with regular serum-free medium for another 16 h. In the last 4 h, cells were pulsed with 1 μCi/ml of [^{3}H]thymidine. In the experiments depicted in B, the inhibitors were added 10 min before ceramide and then readministered after the removal of ceramide from the culture medium. Data are expressed as cpm/50,000 cells. **, $p < 0.01$ versus respective basal value; °°, $p < 0.01$ versus respective ceramide value.

μM, 1 μM, 10 nM, and 100 nM, respectively), caused a moderate but consistent inhibition of the effects of bFGF, ranging between −20 and −30% (Table 1). A much more effective inhibition of the proliferative effects of bFGF was obtained using the MEK inhibitor PD98059 (Table 1), also as reported previously (Florio et al., 1999a). Interestingly, the combined treatment with the inhibitors of the ceramide/NO/cGMP pathway and the PD98059 resulted in a slight but significant additivity. This observation suggests that the two pathways do not converge before the final physiological effect. Indeed, we showed that, on the one hand, the PD98059 compound did not interfere with the NO production induced by bFGF, and, on the other hand, in evaluating ERK1/2 phosphorylation (as an index of ERK1/2 activation), we demonstrated that the NOS inhibitor NNA did not modify the ERK1/2 activation induced by bFGF, suggesting that MAP kinase activity was independent of the NO production (Fig. 12). Moreover, the NO donors SNP (1 μM) and 8-bromo-cGMP (1 μM) did not activate the MAP kinase pathway (Fig. 12), whereas a small activation was observed for SNP and other NO donors only at higher concentrations (10 μM) (data not shown). Thus, under our experimental conditions, the pathways involved in the NO synthesis and ERK1/2 activation do not converge before the final physiological effect.

TABLE 1

Effect of different signal transduction inhibitors on bFGF-induced cell proliferation, in the presence or absence of the MEK inhibitor PD 98059

Data are expressed as percentage of bFGF-induced [^{3}H]thymidine incorporation. Basic FGF caused an increase of 130% over basal [^{3}H]thymidine incorporation ($p < 0.01$).

	–PD98059 (10 μM)	+PD98059 (10 μM)
bFGF (30 ng/ml)	100 ± 8	28.4 ± 1**
bFGF + D609 (20 μM)	70 ± 5.1*	21 ± 1.9**
bFGF + NNA (1 μM)	80 ± 3*	17 ± 2.3**
bFGF + Ly-83583 (10 nM)	71 ± 4.2*	21.2 ± 2.1**
bFGF + KT 5823 (100 nM)	70 ± 4*	22 ± 3**

*, $p < 0.05$;**, $p < 0.01$ versus bFGF.

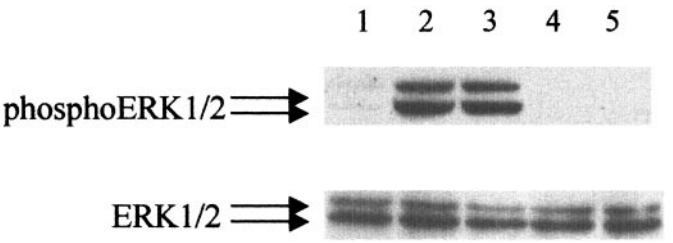

Fig. 12. Activation of ERK1/2 in CHO-K1, measured using a phospho-specific ERK1/2 antibody (top). Equal protein loading was demonstrated by probing the membrane with an antibody directed against the total ERK1/2 proteins (bottom). Lane 1, untreated control cells; lane 2, bFGF (30 ng/ml, 10 min); lane 3, bFGF+NNA (20 μM, 10 min); lane 4, SNP (1 μM, 10 min); lane 5, 8-bromo-cGMP (1 μM, 10 min).

Discussion

In this article, we demonstrate that bFGF is a powerful eNOS activator in CHO-K1 cells via a completely novel intracellular pathway, never described previously for the FGF receptors. Indeed, bFGF caused the activation of eNOS through the regulation of sphingomyelinase activity and the generation of different ceramide species. The role of ceramide in the eNOS activity was also proposed in endothelial cells after bradykinin stimulation (Igarashi et al., 1999). However, in that study, the agonist stimulation was able to induce NO production through the regulation of both the classic Ca^{2+}-dependent and the novel ceramide-related pathways. In CHO-K1 cells bFGF regulates eNOS activity in a completely Ca^{2+}-independent manner. Moreover, this pathway is also independent from other known intracellular pathways previously related to the FGF receptors (PLCγ, phosphatidyl inositol-3 kinase/Akt, and MAP kinase). Conversely, using pharmacological and molecular approaches, we demonstrated that NO synthesis induced by bFGF is dependent on ceramide production. Indeed, two inhibitors of ceramide generation, [i.e., D609 (an inhibitor of PC-PLC) and desipramine (a more specific inhibitor of acidic sphingomyelinase)] completely reversed the effects of bFGF. Moreover, in fibroblasts derived from patients with Niemann-Pick disease, who are genetically deficient for sphingomyelinase, bFGF is completely ineffective; bypassing the genetic defect by administering exogenous ceramide allowed NO production to be restored. Activation of eNOS by bFGF seems to occur inside localized membrane compartments called caveolae. Caveolae are specialized membrane structures reported to represent privileged signal transduction structures (Anderson, 1998). All the components of the metabolic pathway described in this study are highly concentrated in caveolae: caveolae are extremely rich in sphingolipids, from which ceramide is produced (Anderson, 1998), and in acidic sphingomyelinase (Testi, 1996), which seems to participate in the bFGF signaling to generate ceramide. Moreover, in its inactive form, eNOS is selectively sequestered in caveolae through the binding to the main caveolae structural protein, caveolin 1 (Fleming and Busse, 1999). Here, we show that, in resting CHO-K1 cells, eNOS is highly bound to caveolin 1 and that this interaction is disrupted by bFGF treatment in a ceramide-dependent manner. How ceramide is able to favor the translocation and activation of eNOS remains to be determined. It was reported that ceramide is able to activate both serine kinases and phosphatases (Hannun, 1996). In our experimental model, the ceramide-activated protein phosphatase (Dobrowsky and Hannun, 1992) does not seem to be involved because the pretreatment with okadaic acid did not modify the bFGF-dependent NO production (S. Arena, T. Florio and G. Schettini, unpublished results). More recently, it was reported that, in endothelial cells, eNOS activity may be also induced by the ceramide metabolite S1P (Igarashi et al., 2001). S1P is generated through the metabolism of ceramide in sphingosine and its subsequent phosphorylation by specific sphingosine kinases (Spiegel and Merrill, 1996). In turn, newly generated S1P was reported to cause the activation of the EDG subfamily of G-protein-coupled receptors, causing an Akt-dependent phosphorylation of eNOS at Ser^{1179} to stimulate NO production (Igarashi et al., 2001). However, in our cells, despite the significant activation of ceramide synthesis, bFGF does not seem to induce the production of S1P and the consequent activation of Akt and phosphorylation of eNOS. Indeed, the blockade of S1P production, inhibiting the activity of the sphingosine kinase, the inhibition of the EDG receptors by PTX pretreatment, or the blockade of the phosphatidyl inositol-3 kinase/Akt pathway by treatment with wortmannin did not reverse the bFGF-dependent NO production. Thus, in our experimental model, eNOS activation by bFGF seems to be directly regulated by the ceramide forma-

tion, without the involvement of S1P synthesis and the activation of the EDG receptors. A similar regulation was also reported for the NO synthesis induced by the B2 bradykinin receptors. Indeed, in endothelial cells, bradykinin activates eNOS through ceramide production (Igarashi et al., 1999) without activation of the S1P intracellular pathway, because, unlike S1P, bradykinin does not cause the activation of Akt and the phosphorylation of eNOS (Igarashi et al., 2001). Using the CHO-K1 cell line, another pathway involved in the NO generation through the CCK-A receptor was also described previously (Cordelier et al., 1999). In particular, it was reported that CCK was able to activate nNOS through tyrosine dephosphorylation of the enzyme mediated by the tyrosine phosphatase SHP2 (Cordelier et al., 1999). In our experiments, we confirmed the presence of both eNOS and nNOS isoforms in CHO-K1 cells, as also observed by the previous report (Cordelier et al., 1999). However, we demonstrated that the activation of a different family of membrane receptors (i.e., tyrosine kinase versus G-protein-coupled) is able to regulate the NOS activity through a completely distinct mechanism. Interestingly, the pretreatment with vanadate, which completely reverses the CCK-induced NO production (Cordelier et al., 1999), does not interfere with the eNOS activation by bFGF (S. Arena, T. Florio, and G. Schettini, unpublished observation). Thus, in the same cell type, the activation of two different classes of receptors causes the activation of different NOS isoforms through completely independent pathways. However, the final physiological effect of the NO, and the subsequent cGMP production induced by both bFGF and CCK, is the proliferation of CHO-K1 cells (current study; Cordelier et al., 1997). Indeed, although often regarded as degenerative agents, both NO and ceramide may be, depending on the intracellular levels and the time of exposure, important proliferative agents (Olivera et al., 1992; Cordelier et al., 1997). Different effectors, however, are involved in these effects; the NO/cGMP synthesis induced by CCK was reported to directly regulate the ERK1/2 pathway to induce cell proliferation (Cordelier et al., 1997) whereas, in our experiments, NO and cGMP do not modify ERK1/2 activation induced by bFGF. The relationship between NO and ERK activation is still very controversial also in other cell systems. For example, in vascular smooth muscle cells, NO and cGMP inhibit ERK1/2 phosphorylation/activation (Mitani et al., 2000). However, it is still unclear how, in CHO-K1 cells, NO generated in different ways (through eNOS by bFGF or through nNOS by CCK) may result in a diverse regulation of ERK activity, although in both cases it causes a proliferative effect.

In our experiments, NO/cGMP generation contributes to only a small percentage of the proliferative effects of bFGF, which, conversely, are at least 70% dependent on the ERK1/2 activation. This small effect allows us to hypothesize that in more specialized cells, growth factor-dependent NO production may be involved in more differentiated functions.

A recent report showed that in rat astrocytes, proliferation was associated with a decrease in ceramide production (Riboni et al., 2001). This observation, taken together with the growing bulk of articles showing either antiproliferative and apoptotic or proliferative effects of ceramide and NO in different cell systems, indicates that a careful evaluation of cell-specific responses to ceramide generation is mandatory.

In conclusion, we describe a completely novel intracellular pathway by which growth factor receptors, in particular FGF receptors, induce NO and cGMP synthesis. We report that, in CHO-K1 cells, FGF receptor activation is able to regulate the synthesis of ceramide that causes activation of the eNOS. Moreover, the NO/cGMP pathway activation causes an ERK1/2-independent proliferative effect.

Acknowledgments

We are thankful to G. Contento for technical assistance in cGMP measurements. We thank the Laboratorio di Diagnosi PrePostnatale Malattie Metaboliche (Istituto G. Gaslini, Genova, Italy) for providing us with specimens from the collection "Cell lines and DNA bank from patients affected by Genetic diseases", supported by TELETHON grants.

References

Albouz S, Vanier M, Hauw J, Le Saux F, Boutry J, and Baumann N (1983) Effect of tricyclic antidepressant on sphingomyelinase and other sphingolipid hydrolases in C6 cultured glioma cells. *Neurosci Lett* **36:**311–315.

Anderson RGW (1998) The caveolae membrane system. *Annu Rev Biochem* **67:**199–225.

Bradford MM (1976) A rapid and sensitive method for the quantitation of microgram quantities of protein utilizing the principle of protein-dye binding. *Anal Biochem* **72:**248–254.

Brenman JE, Chao DS, Gee SH, McGee AW, Craven SE, Santillano DR, Wu Z, Huang F, Xia H, Peters MF, et al. (1996) Interaction of nitric oxide synthase with the postsynaptic density protein PSD-95 and α1-syntrophin mediated by PDZ domains. *Cell* **84:**757–767.

Cifone MC, Roncaioli P, De Maria R, Camarda G, Santoni A, Ruberti G, Testi R (1995) Multiple pathways originate at the Fas/APO-1 (CD95) receptor: sequential involvement of phosphatidyl choline-specific phospholipase C and acidic sphingomyelinase in the propagation of the apoptotic signal. *EMBO (Eur Mol Biol Organ) J* **14:**5859–5868.

Cordelier P, Esteve J-P, Bousquet C, Delesque N, O'Carroll A-M, Schally AV, Vaysse N, Susini C, and Buscail L (1997) Characterization of the antiproliferative signal mediated by the somatostatin receptor subtype sst5. *Proc Natl Acad Sci USA* **94:**9343–9348.

Cordelier P, Esteve J-P, Rivard N, Marletta M, Vaysse N, Susini C, and Buscail L (1999) The activation of neuronal NO synthase is mediated by G-protein $\beta\gamma$ subunit and the tyrosine phosphatase SHP-2. *FASEB J* **13:**2037–2050.

Corson MA, James ML, Latta SE, Nerem RM, Berk BC, and Harrison DG (1996) Phosphorylation of endothelial nitric oxide synthase in response to fluid shear stress. *Circ Res* **79:**984–991.

Dobrowsky RT and Hannun YA (1992) Ceramide stimulates a cytosolic protein phosphatase. *J Biol Chem* **267:**5048–5051.

Edsall LC, Van Brocklyn JR, Cuvillier O, Kleuser B, and Spiegel S (1998) *N, N*-Dimethylsphingosine is a potent competitive inhibitor of sphingosine kinase but not of protein kinase C: modulation of cellular levels of sphingosine 1-phosphate and ceramide. *Biochemistry* **37:**12892–12898.

Feron O, Belhassen H, Kobzik L, Smith TW, Kelly RA, and Michel T (1996) Endothelial nitric oxide synthase targeting in caveolae: specific interaction with caveolin isoforms in cardiac monocytes and endothelial cells. *J Biol Chem* **271:**22810–22814.

Fleming I and Busse R (1999) Signal transduction of eNOS activation. *Cardiovasc Res* **43:**532–541.

Florio T, Yao H, Carey KD, Dillon TJ, and Stork PJS (1999a) Somatostatin activation of MAP kinase via somatostatin receptor 1 (SSTR1). *Mol Endocrinol* **13:**24–37.

Florio T, Thellung S, Arena S, Corsaro A, Spaziante R, Gussoni G, Giusti M, Giordano G, and Schettini G (1999b) Somatostatin and its analogue lanreotide inhibit the proliferation of dispersed human non-functioning pituitary adenoma cells, *in vitro*. *Eur J Endocrinol* **141:**396–408.

Folch J, Less M, and Stanley HS (1957) A simple method for the isolation and purification of total lipids from animal tissues. *J Biol Chem* **226:**497–509.

Folkman J (1995) Clinical applications of research on angiogenesis. *N Engl J Med* **333:**1757–1763.

Garcia-Cardena G, Fan R, Stern D, Liu J, and Sessa WC (1996) Endothelial nitric oxide synthase is regulated by tyrosine phosphorylation and interacts with caveolin 1. *J Biol Chem* **271:**27237–27240.

Grynkiewicz G, Poenie M, and Tsien RY (1985) A new generation of calcium indicators with greatly improved fluorescence properties. *J Biol Chem* **260:**3440–3450.

Hannun YA (1996) Functions of ceramide in coordinating cellular responses to stress. *Science (Wash DC)* **274:**1855–1859.

Igarashi J, Bernier SG, and Michel T (2001) Sphingosine 1-phosphate and activation of endothelial nitric oxide synthase. Differential regulation of Akt and MAP kinase pathways by EDG and bradykinin receptors in vascular endothelial cells. *J Biol Chem* **276:**12420–12426.

Igarashi J, Thatte HS, Prabhakar P, Golan DE, and Michel T (1999) Calcium-independent activation of endothelial nitric oxide synthase by ceramide. *Proc Natl Acad Sci USA* **96:**12583–12588.

Kalhorn T and Zager RA (1999) Renal cortical ceramide patterns during ischemic and toxic injury: assessments by HPLC-mass spectrometry. *Am J Physiol* **277:**F723–F733.

Koeck T and Kremser K (2001) Peroxisomal deficiencies are associated with altered activity of endothelial NOS in human fibroblasts. *Nitric Oxide* **5:**213–216.

Kolesnick R and Fuks Z (1995) Ceramide: a signal for apoptosis or mitogenesis? *J Exp Med* **181:**1949–1952.
Mitani Y, Zaidi SH, Dufourq P, Thompson K, and Rabinovitch M (2000) Nitric oxide reduces smooth muscle cell elastase activity through cGMP-mediated suppression of ERK phosphorylation and AML1B nuclear partitioning. *FASEB J* **14:**805–814.
Moncada S and Higgs A (1993) The L-arginine nitric oxide pathway. *N Engl J Med* **329:**2002–2012.
Moncada S, Palmer RM, and Higgs EA (1991) Nitric oxide: physiology, pathophysiology and pharmacology. *Pharmacol Rev* **43:**109–142.
Montagnani M, Chen H, Barr VA, and Quon MJ (2001) Insulin-stimulated activation of eNOS is independent of Ca^{2+} but requires phosphorylation by Akt at $Ser^{(1179)}$. *J Biol Chem* **276:**30392–30398.
Nathan C and Xie Q (1994) Nitric oxide synthases: roles, tolls and controls. *Cell* **78:**915–918.
Olivera A, Buckley NE, and Spiegel S (1992) Sphingomyelinase and cell-permeable ceramide analogs stimulate cellular proliferation in quiescent Swiss 3T3 fibroblasts. *J Biol Chem* **261:**26121–26127.
Rees DD Palmer RM, Schulz R, Hodson H and Moncada S (1990) Characterization of three inhibitors of endothelial nitric oxide synthase in vitro. *Br J Pharmacol* **101:**746–752.
Riboni L, Viani P, Bassi R, Giussani P, and Tettamanti G (2001) Basic fibroblast growth factor-induced proliferation of primary astrocytes. Evidence for the involvement of sphingomyelin biosynthesis. *J Biol Chem* **276:**12797–12804.
Schmidt NO, Westphal M, Hagel C, Ergun S, Stavrou D, Rosen EM, and Lamszus K (1999) Levels of vascular endothelial growth factor, hepathocyte growth factor/scatter factor and basic fibroblast growth factor in human gliomas and their relation to angiogenesis. *Int J Cancer* **84:**10–18.
Spiegel S and Merrill AH Jr (1996) Sphingolipid metabolism and cell growth regulation. *FASEB J* **10:**1388–1397.
Spiegel S and Milstien S (2000) Functions of a new family of sphingosine 1-phosphate receptors. *Biochim Biophys Acta* **1484:**107–116.
Spoto G, Whitehead E, Ferraro A, Di Terlizzi PM, Turano C, and Riva F (1991) A reverse-phase HPLC method for cAMP phosphodiesterase activity. *Anal Biochem* **196:**207–210.
Szabo C, Southan GJ, and Thiemermann C (1994) Beneficial effects and improved survival in rodent models of septic shock with S-methylisothiourea sulphate, a potent and selective inhibitor of inducible nitric oxide synthase. *Proc Natl Acad Sci USA* **91:**12472–12476.
Testi R (1996) Sphingomyelin breakdown and cell fate. *Trends Biol Sci* **21:**468–471.
Thellung S, Florio T, Maragliano A, Cattarini G, and Schettini G (1999) Polydeoxyribonucleotides enhance the proliferation of human skin fibroblasts: involvement of A_2 purinergic receptor subtypes. *Life Sci* **64:**1661–1674.
Wang E, Norred WP, Bacon CW, Riley RT, and Merrill AH Jr (1991) Inhibition of sphingolipid biosynthesis by fumonisins. Implications for diseases associated with Fusarium moniliforme. *J Biol Chem* **266:**14486–14490.
Ziche M, Morbidelli L, Choundouri R, Zhang HT, Donnini S, Granger HJ, and Bicknell R (1997) Nitric oxide synthase lies downstream from vascular endothelial growth factor-induced but not basic fibroblast growth factor-induced angiogenesis. *J Clin Investig* **99:**2625–2634.

Address correspondence to: Prof. Tullio Florio, Unità Neuroscienze, Centro Biotecnologie Avanzate, Largo Rosanna Benzi 10, 16132 Genova, Italy. E-mail: florio@cba.unige.it